



# Correlation effects in mass-asymmetric electron-hole plasmas

V.S. Filinov<sup>1,2</sup>, V. Fortov<sup>1</sup>, P. Levashov<sup>1</sup>, M. Bonitz<sup>2</sup>, and H. Fehske<sup>3</sup>

<sup>1</sup>Institute for High Energy Density, Russian Academy of Sciences, Moscow, Russia

<sup>2</sup>Institut für Theoretische Physik und Astrophysik, Christian-Albrechts-Universität zu Kiel, Germany

<sup>3</sup>Institut für Physik, Ernst-Moritz-Arndt-Universität Greifswald, Germany



**Abstract:** The fraction of the electron-hole and hole-hole bound states, pair correlation functions, snapshots of the particle positions, internal energy and equation of state of a mass-asymmetric electron-hole plasma are determined by direct path integral Monte Carlo simulations. Data for the isotherms  $T=30-300$  K are presented. Density-temperature regions have been found for existence of the excitons, bi-excitons and many-particle clusters. The transition to a metallic state is detected. Results are discussed in relation to the excitonic phase diagram of  $TmSe_{0.45}Te_{0.55}$ .

## Motivation

In [1] thermodynamic properties of the condensed excitonic phase of the intermediate valent system  $TmSe_{0.45}Te_{0.55}$  have been measured between 1.5 K and 300 K and ambient pressure between 1.7 kbar and 17 kbar, as a first experiment of its kind.

Fig. 1 shows the temperature-pressure diagram of the condensed excitonic phase. At temperatures above about 250 K one crosses with increasing pressure between 10 and 11 kbar the (short)-dashed line, separating the semi-conductor and semi-metallic phases. At lower temperatures instead, one enters with increasing pressure first the condensed excitonic state (above 5 kbar) and leaves after the excitonic state to enter the semi-metallic phase. Such a behaviour has been predicted by Mott and Kohn [2].

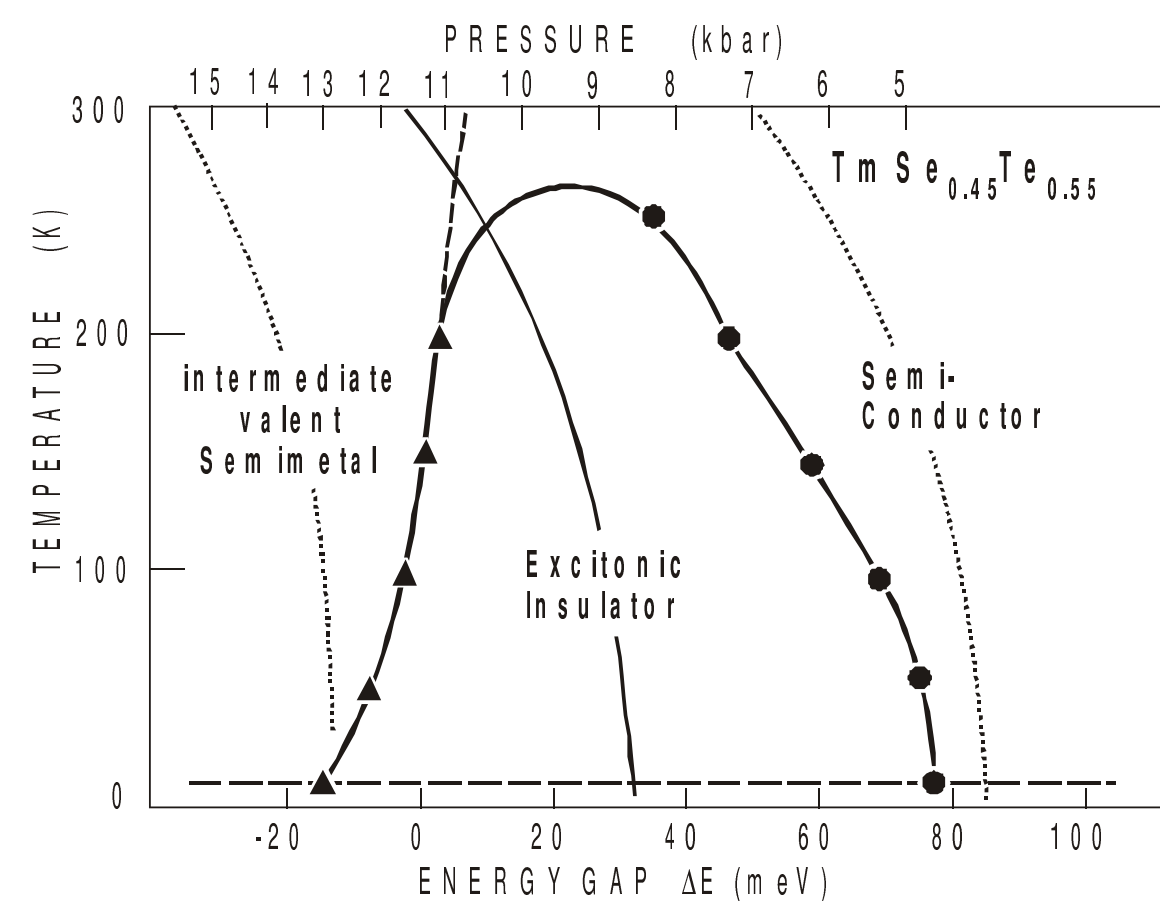


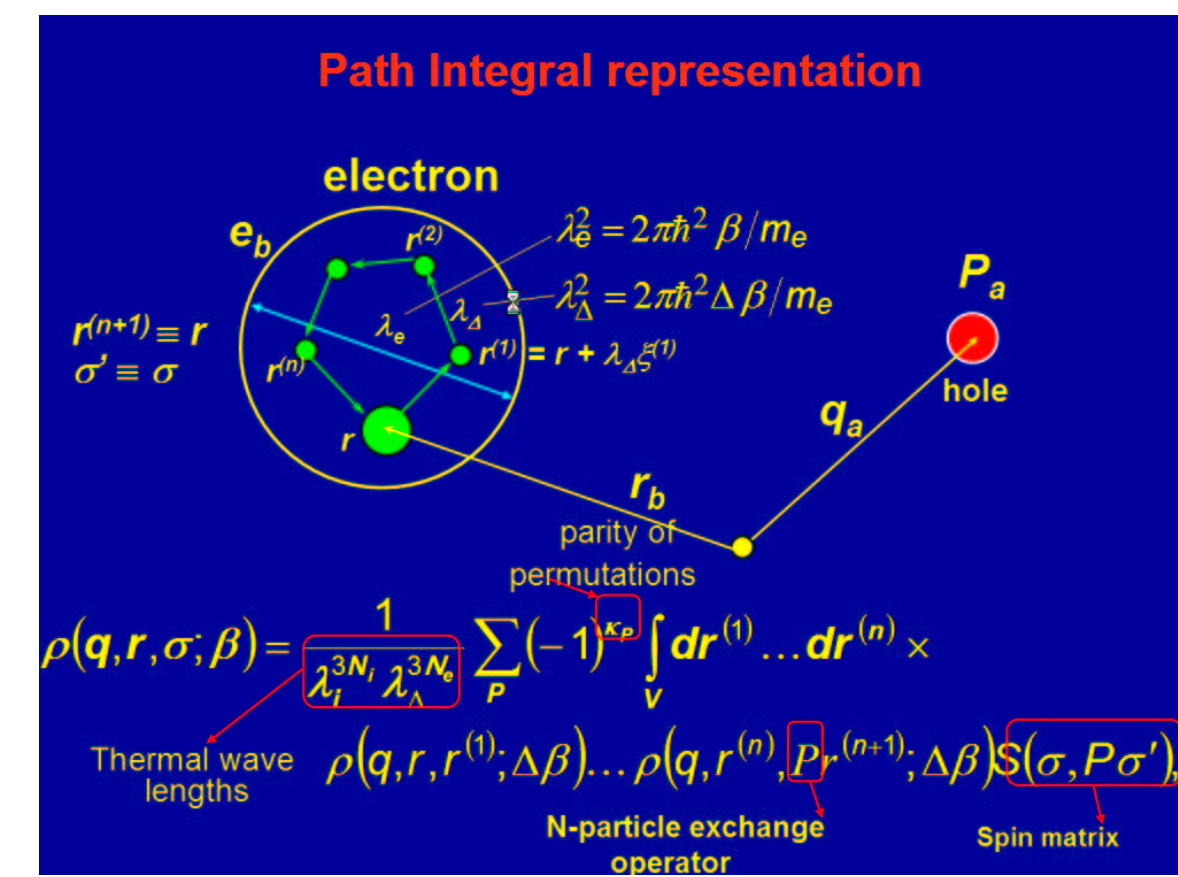
Fig. 1 Excitonic phase diagram of  $TmSe_{0.45}Te_{0.55}$  taken from [1]. Experimental points designated by symbols. "Isobars" in the semi-conducting and semi-metallic phase are shown as dotted lines, whereas an "isobar" entering the excitonic phase is shown by a full line. In the lower abscissa the energy gap  $\Delta E$  is plotted (negative values refer to the metallic state).

## Model & Simulation Idea

- Direct Path Integral Monte Carlo (DPIMC) simulations of a (quantum) plasma [3] with  $N_e$  electrons and  $N_h$  holes
- Kelbg potential for Coulomb particles
- Input from experiments: effective masses  $m_e = 2$ ,  $m_h = 80$  and permittivity  $\epsilon \approx 20 \dots 25$  ( $E_b = 517K$ ).

**Quantum Monte Carlo method**  
**Canonical ensemble**

- Binary mixture of  $N_e$  electrons and  $N_h$  holes
- Partition function:  
 $Z(N_e, N_h, V, \beta) = Q(N_e, N_h, \beta) / N_e! N_h!$   
 $Q(N_e, N_h, \beta) = \int \prod d\mathbf{r} \rho(\mathbf{q}, \mathbf{r}, \sigma, \beta) / N_e! N_h!$
- N-particle density matrix:  
 $\rho = \exp(-\beta H) = \exp(-\Delta\beta H) \times \dots \times \exp(-\Delta\beta H)$   
 $\beta = 1/kT$   
 $\Delta\beta = \beta / (n+1)$



**«Sign problem»**

$$\rho(\mathbf{q}, \mathbf{r}, \sigma, \beta) = \frac{1}{Z} \sum_{\mathbf{r}'} \rho_s(\mathbf{q}, [\mathbf{r}'] | \beta)$$

$$\rho_s(\mathbf{q}, [\mathbf{r}'] | \beta) = \frac{C_N}{2^N} \exp[-\beta U(\mathbf{q}, [\mathbf{r}'] | \beta)] \prod_{i=1}^N \phi_{\beta p} \det |\psi_{ab}^{ij}|_s$$

Coulomb potential:  $U(\mathbf{q}, [\mathbf{r}'] | \beta) = U^e(\mathbf{q}) + \sum_{i=1}^n U^h([\mathbf{r}'] | \beta) + U^p(\mathbf{q}, [\mathbf{r}'] | \beta)$

Exchange matrix:  $|\psi_{ab}^{ij}|_s = \left| \exp\left\{ \frac{\pi}{\lambda_{ab}} (r_a - r_b) + y \beta^2 \right\} \right|_s$

**Kelbg potential**

$$\Phi_{ab}^{ij}(\mathbf{r}_{ab}, \Delta\beta) = \frac{e^{-\epsilon \epsilon_{ij}}}{\lambda_{ab} x_{ab}} \left\{ 1 - e^{-x_{ab}} + \sqrt{\pi} x_{ab} [1 - \text{erf}(x_{ab})] \right\}$$

where  $x_{ab} = |r_{ab}| / \lambda_{ab}$ ,  $\lambda_{ab} = 2\pi\hbar^2 \beta / \mu_{ab}$

## Numerical Results

### Fraction of Bound States

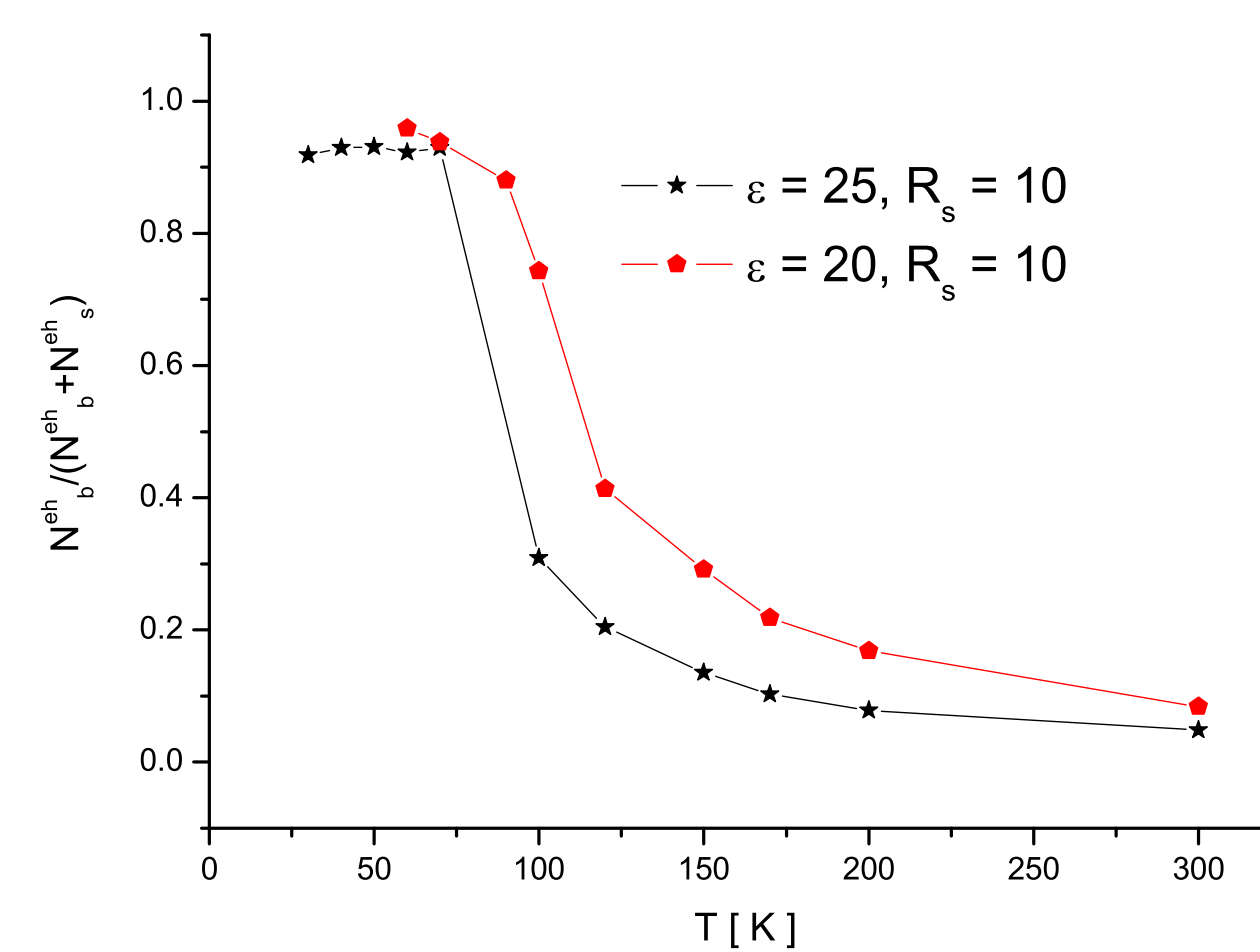


Fig. 2: Fraction of the electron-hole bound states vs temperature.

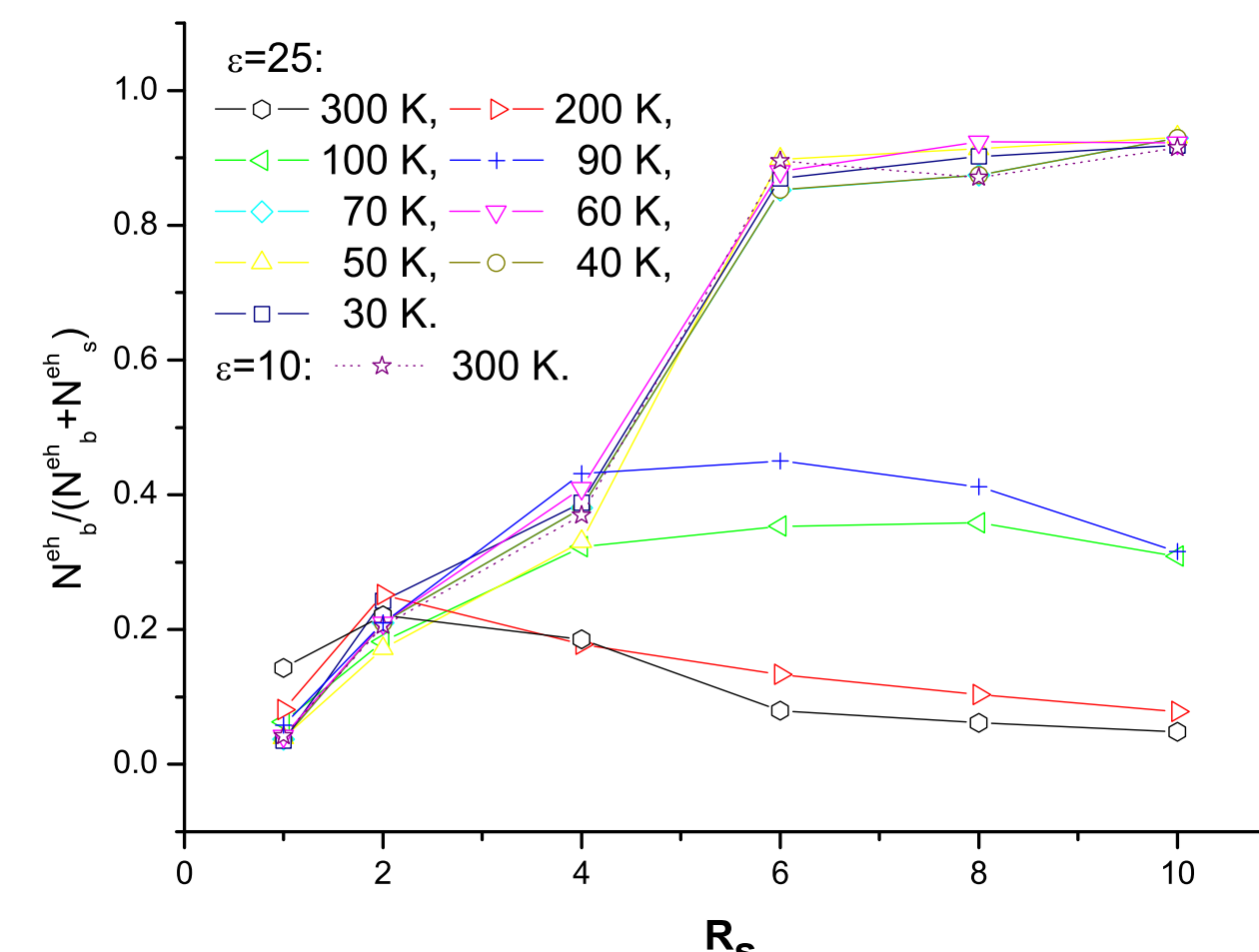


Fig. 3: Fraction of the electron-hole bound states vs Brueckner parameter.

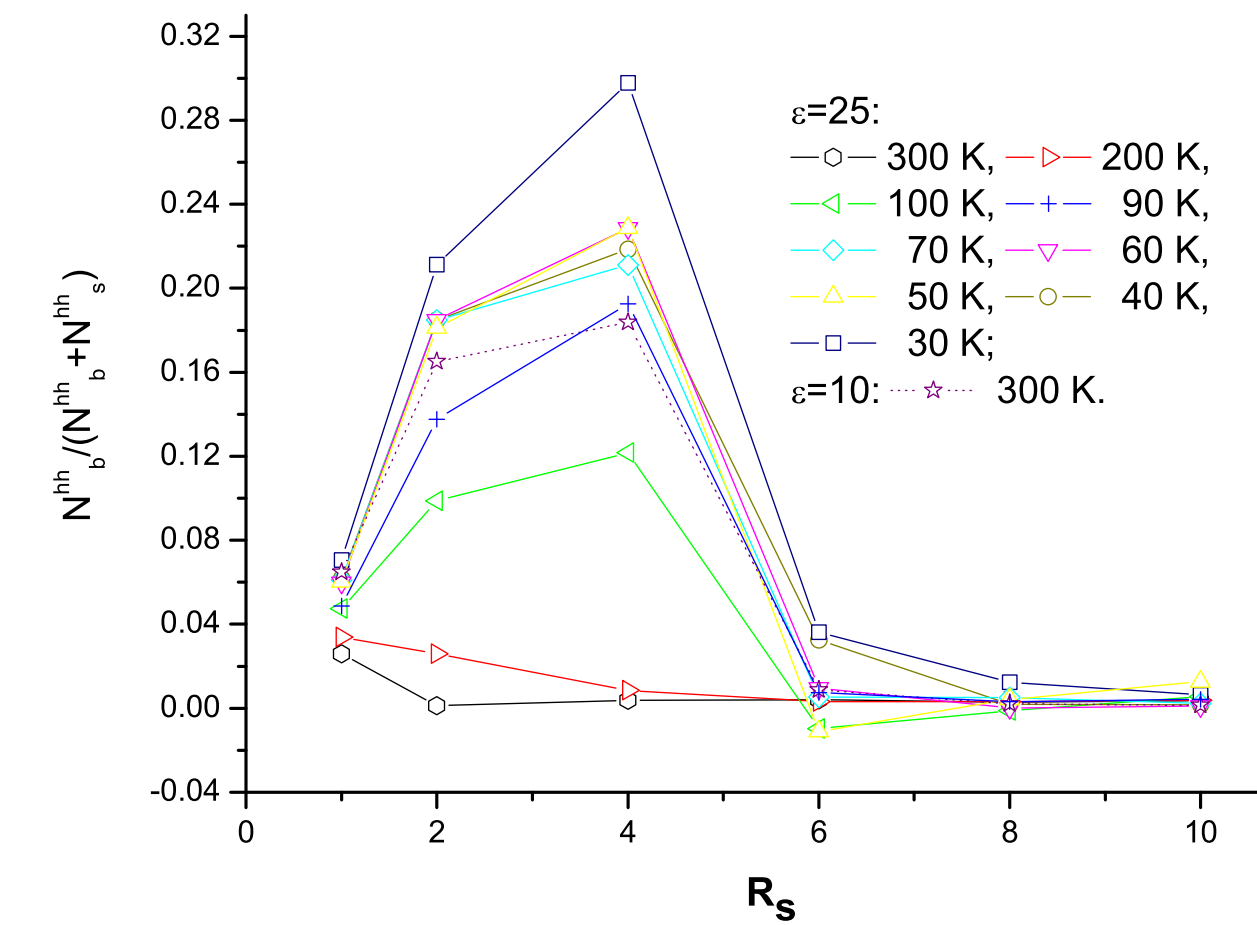


Fig. 4: Fraction of the hole-hole bound states vs Brueckner parameter

## Typical Snapshots

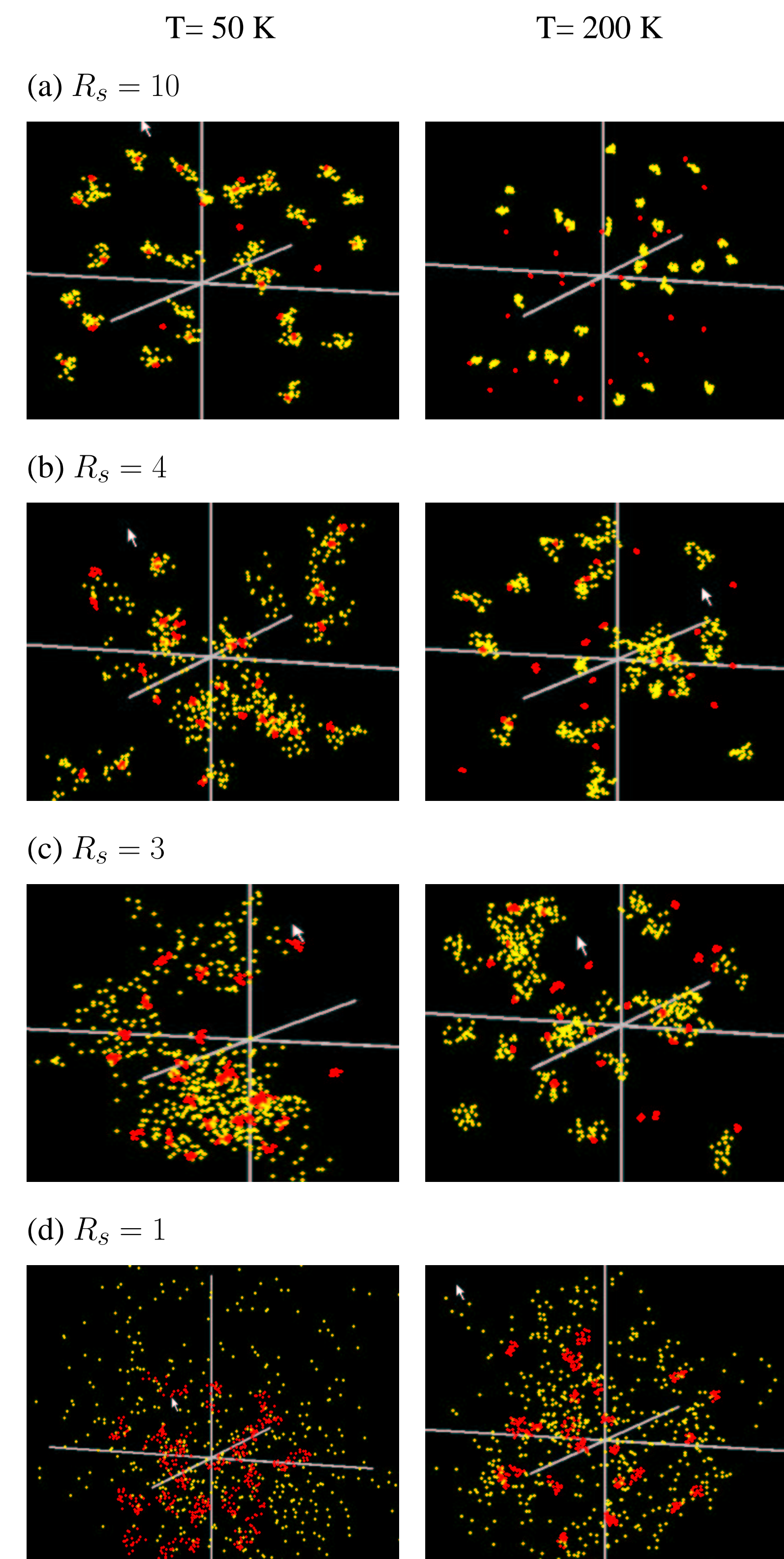


Fig. 5: DPIMC simulations of the strongly correlated quantum electron-hole plasma at different Brueckner parameters  $R_s$ . Electrons and holes are shown by (clouds of) yellow and red dots, respectively. At low temperatures one observes the formation of tightly bound well-separated excitons (a), bi-excitons (b), clusters (c), and a "hole-fluid" (d). At high temperatures a "dissociation" of the several bound states takes place; as a result an ionised electron-hole plasma is formed.

## Pressure and Internal Energy

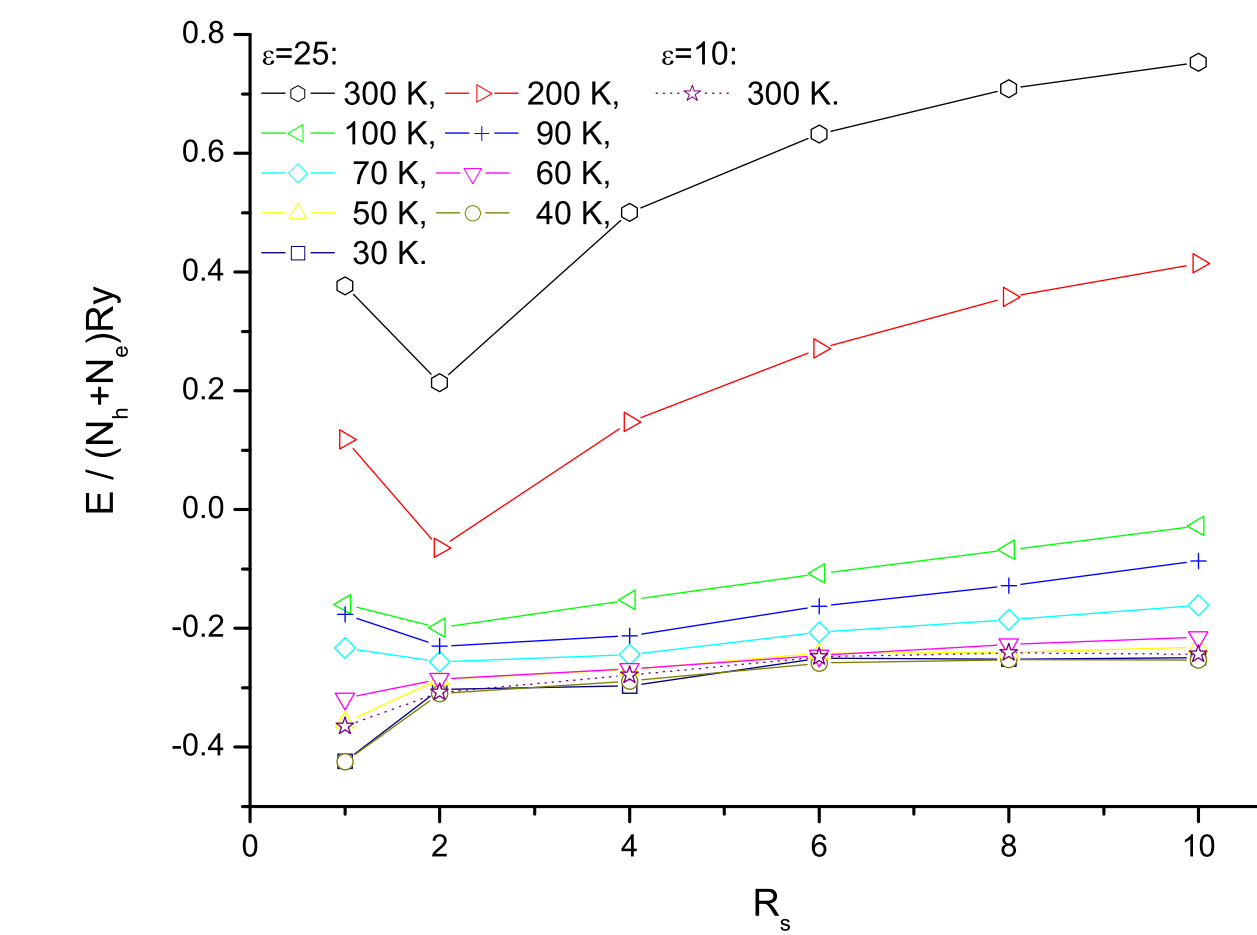


Fig. 6: Coulomb interaction (Fermi repulsion) between particles leads to a lowering (increase) of the energy at  $R_s > 2$  ( $R_s < 2$ ).

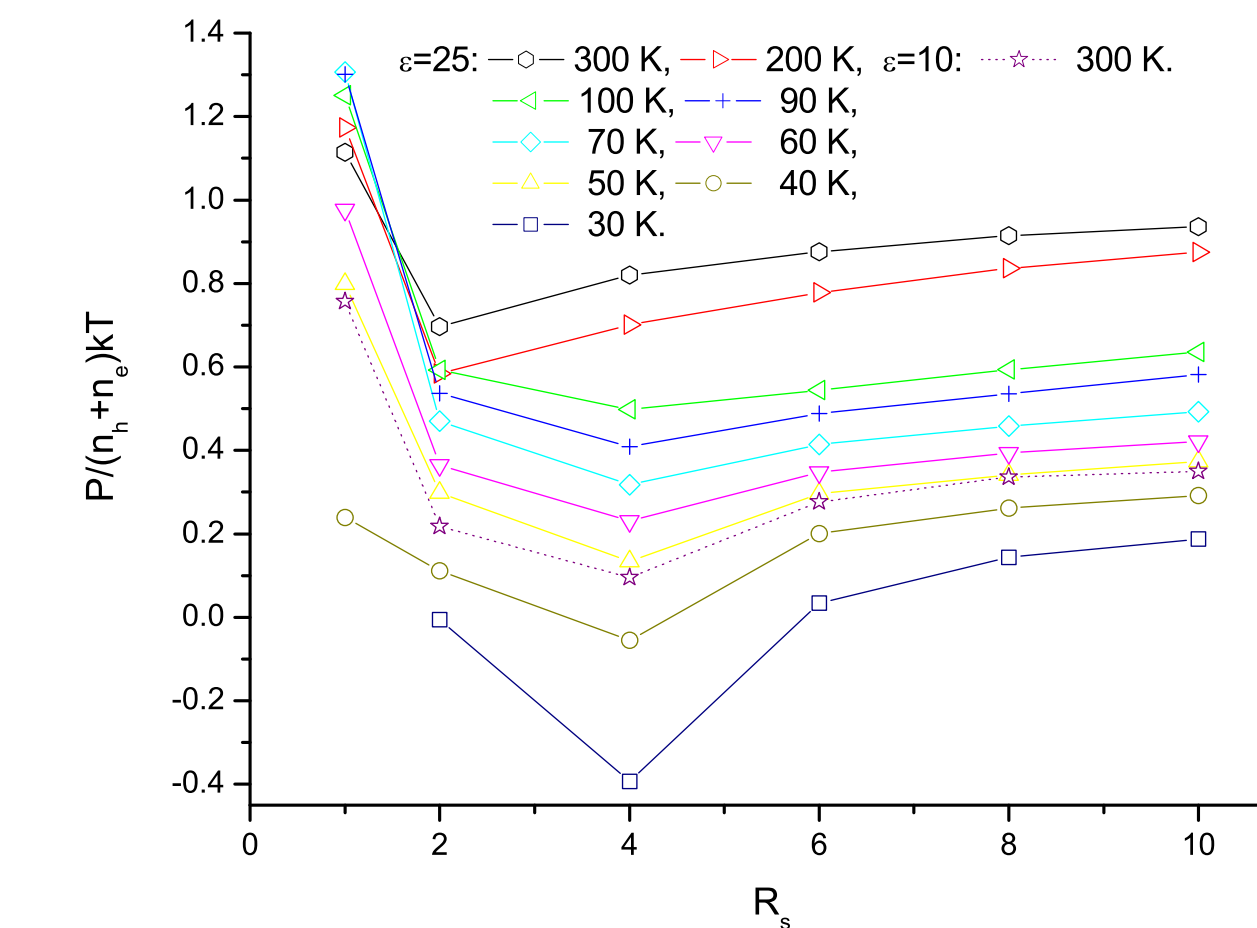


Fig. 7: Coulomb interaction (Fermi repulsion) between particles leads to a lowering (increase) of pressure at  $R_s \sim 3$  ( $R_s \leq 3$ ).

## Pair Correlation Functions

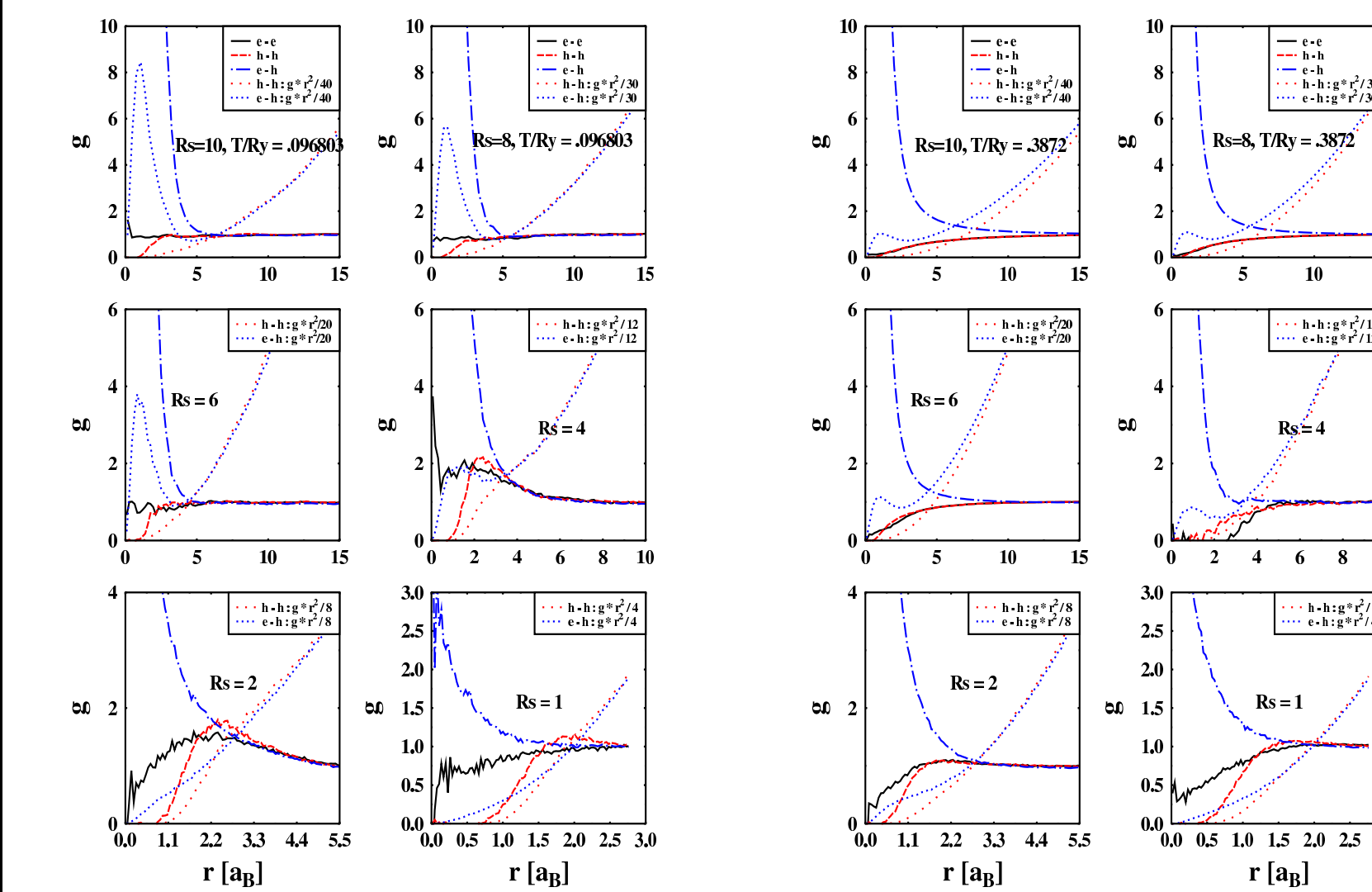


Fig. 8: Pair correlation functions at  $T=50$  K and  $T=200$  K. Distance between particles is given in Bohr radii.

## Discussion

Let us first discuss the general behaviour of an electron-hole plasma at high temperatures. It is well-known that the energy of an ideal plasma increases with increasing density. The increase is particularly strong at high densities due to (electron) degeneracy effects. The non-ideal electron-hole plasma, on the other hand, shows a significant deviation from this trend: the formation of an energy minimum at intermediate densities (in full agreement with the existing analytical predictions). Our non-ideal plasma data asymptotically approaches the standard results at low density (ideal classical plasma) and at high density (ideal mixture of classical holes and quantum electrons). At intermediate densities, between  $R_s = 6$  and  $R_s = 1$ , the energy of the non-ideal plasma is notably lower than that of an ideal plasma, mainly due to strong correlations and formation of bound states. With decreasing temperature this region broadens. Most

notably, for the considered temperatures, the pressure becomes negative, indicating an instability.

In the region of a possible plasma phase transition ( $R_s \sim 3$ ), we observe large fluctuations of pressure and energy related to formation and decay of many-particle clusters. Furthermore, there are significant surface energy effects as our simulations yield just a very small number of clusters (typically one to three), each containing 15 to 50 electron-hole pairs. To clarify this interesting issue in more detail requires, however, further extensive simulations with substantially larger particle numbers.

As an effect of the Coulomb repulsion, the pair correlations  $g_{ee}$  and  $g_{hh}$  decay at small distances. The decay of the electron-electron correlations is essentially different from that of the hole-hole correlations due to the large mass difference. In the electron subsystem, quantum exchange and tunnelling compete with the Coulomb repulsion.

Let us emphasise the qualitatively different physical behaviour at high and low temperatures, e.g.  $T=50$  K and  $T=200$  K. Note that  $R_s = 10$  corresponds to the case of weak coupling, while  $R_s = 1$  relates to strong coupling and strong degeneracy. In case of low temperature and high density the electron-electron and hole-hole pair distribution functions show distinct peaks close to  $r = 2a_B$  and  $4a_B$ , pointing towards the formation of bi-excitons and many-particle clusters, respectively. The strong peak of  $g_{eh}$  (note the scale) is caused by excitons. This is confirmed by considering  $r^2 g_{eh}(r)$  which is peaked around  $a_B$ . At high temperatures and/or high densities  $g_{ee}$ ,  $g_{hh}$  and  $r^2 g_{eh}$  exhibit no peak structure, i.e. there is no indication for bound states.

Next let us discuss the existence of excitons at  $T = 50$  K varying the density over 3 orders of magnitude. As a matter of course, the highest peak of  $r^2 g_{eh}$  is observed for  $R_s = 10$ . For density  $R_s = 6$  it is decreased due to the recombination into bi-excitons. At still higher densities, the excitonic fraction is reduced further due to many-body effects (pressure ionisation). Interestingly, for densities above  $R_s = 6$ , the excitonic peak of  $r^2 g_{eh}$  shifts from approximately  $a_B$  to about  $3a_B$ . This can be traced back to a variety of effects, but predominantly to the increased bi-excitonic fraction, which favours a broad peak of  $r^2 g_{eh}$  in the range from  $r \approx a_B$  to  $r \approx 3a_B$ .

Finally, at  $R_s = 1$ , the molecules have vanished, and the electron-hole function again shrinks and the peak-structure disappears. Note that this density is close to the Mott density. A further increase of the density destroys the remaining excitons completely. It is interesting to compare the shape of the peak of  $r^2 g_{eh}$  to that of the ground state wave function. While at low densities the simulation peaks are broader, indicating the population of excited states and bi-excitons, at high densities ( $R_s \sim 1$ ) we observe that the maximum is significantly narrower than the ground state peak. Hence the pair hole-hole correlation functions reveal at about  $R_s \sim 1$  an ordering of the holes into a fluid-like state.

**Summary:** Our simulations revealed an instability of the homogeneous plasma state around the minimum of the energy isotherm for densities around  $R_s \sim 3$ . We found evidence that this might be due to cluster formation. The appearance of these clusters gives strong indication for a first-order phase transition from an (excitonic) insulator phase to a semi-metal. Clearly such plasma phase transition would have drastic consequences for transport properties. Finally, at high density,  $R_s \sim 2$ , our simulations revealed ordering of the holes into a liquid like fluid state.

## References

- [1] P. Wachter, B. Bucher, and J. Malar, Phys. Rev. B **69**, 094502 (2004).
- [2] N. Mott, Philos. Mag. **6**, 287 (1961); W. Kohn, in *Many Body Physics*, edited by C. de Witt and R. Bailian (Gordon & Breach, New York, 1968).
- [3] A. Filinov, M. Bonitz, and W. Ebeling, J. Phys. A: Math. Gen. **36** (2003).